Scale-Free Dynamics of Brain Network Activity in Mice During Novelty and Exploration.

Mihaela Dimitrova Gerova
s1029809

Supervisor: dr Michael X Cohen
First reader: dr Arthur de Franca
Second reader: dr Bernhard Englitz

Abstract: The brain is considered a "critical system," which continuously transitions between two phases: in one the neural activity amplifies and spreads over the largest distances in the network, and in the other the neural activity is reduced and localized. A strong indication that a system is in a critical state is scale-free behaviour, which is best described by the exponent of a power-law function. This scaling exponent can be obtained from Demeaned Fluctuation Analysis (DMA), and indicates in which state the system is. In this study, we analyzed local field potential (LFP) recordings from the hippocampal-cortical network in 6 mice during an object recognition task, and DMA was applied for frequencies from 2 Hz to 150 Hz to identify neural oscillations and regions indicating above-noise level scaling exponents for each experimental stage. Our results suggest that there is a significant increase of hippocampal scaling exponents in beta (24-29 Hz) associated with novelty and exploration compared to rest. We also found evidence suggesting that different CA1 hippocampal sides might be contributing differently to the scaling properties of theta (4-7 Hz) associated with novelty detection. We hypothesize that scaling dynamics in theta might be reflecting coordination of information in the hippocampal-cortical network during object recognition. The greatest variability in scaling dynamics was observed in gamma (96-102) in the parietal cortex during object exploration. We therefore hypothesize that parietal gamma scaling dynamics reflect a rather general mechanism involved in the task. Overall, our results suggest that the scaling dynamics of different frequency bands can be linked to behavioral outcomes, and reflect different processes involved in the object recognition task.

Keywords: Demeaned Fluctuation Analysis, Criticality, Scaling Exponents, LFP, Object Exploration, Novelty.

Introduction

Criticality: Origins

The theory of self-organized criticality (SOC) was first introduced by Per Bak (1987, 1988). In the last few decades SOC has significantly influenced the development of complexity science, and has found applications in numerous fields (Watkins et al., 2016). This framework describes systems which undergo a phase transition at a special state, often described by a single parameter such as temperature or pressure.

A strong indication of a critical system operating at a phase transitioning point is scale-free behavior. Scale-free phenomena are best described by the exponent of a power law function, because it best captures the relationship between fluctuations on different scales (Hardstone et al., 2012). This means that the output of a critical system cannot be described by a single scale. Numerous natural phenomena, such as earthquakes (Christensen et al., 2002), forest fires (Malamud et al., 1998), and sand pile avalanches (Carlson et al., 1990) are best described by a power law distribution and are therefore believed to be the result of a critical process. In time series, power law means that signal power is inversely proportional to its frequency, and is often referred to as 1/f noise.

Criticality and the Brain

There is a growing evidence that diverse non-linear multi-unit systems tend to self-organize towards criticality to form spatiotemporal long-range correlations (Bak et al., 1988; Usher et al., 1995). The mechanism hypothesized to lead to self-tuning towards criticality is that the interactions between different units on a local level undergoes activity-induced changes, which in turn accumulate to form the system's memory (Maslov et al., 1994). There is also evidence suggesting that similar processes are present in neural systems (K. Linkenkaer-Hansen et al., 2001; Pritchard, 1992; Ville et al., 2010).

The first piece of empirical evidence supporting the critical brain hypothesis comes from neural avalanches, which are defined as a series of consecutively firing neurons or consecutively activated electrodes, preceded and followed by inactivity (Beggs & Plenz, 2003; Friedman et al., 2012). Beggs and Plenz (2003) measured spontaneous activity from cultured and acute slices from mice cortex, and found that the probability of an avalanche occurring of a given size is characterized by a power law, and these results were robust to the discrete interval of measurement.

Theoretical and computational models show that under criticality, memory is enhanced, resources are optimized, and a neuronal system will be most efficient in information communication (Beggs & Plenz, 2003). Shew and colleagues (2009) studied the dynamic range of cortical networks, defined by the range of responses to stimulus intensities, and showed that the dynamic range is maximized under an intermediate excitation-inhibition ratio, when neuronal avalanches are occurring. In another study, the authors from the same research group showed that information capacity and mutual information are optimized under the intermediate excitation-inhibition ratio (Shew et al., 2011). Altogether, these studies outline the functional significance of criticality in the brain.

Most of the research exploring criticality dynamics in humans is based on the analysis of spontaneous oscillatory activity, and comparing these dynamics between health and disease. It has been shown that in numerous mental conditions such as Alzheimer's (Jiang et al., 2018; Maxim et al., 2005), Schizophrenia (Moran et al., 2019) , Major Depressive Disorder (Klaus Linkenkaer-Hansen et al., 2005), and Autism (Lai et al., 2010) brain patterns are deviating from criticality either on a global scale, or in specific regions when compared to controls. It has been thus hypothesized that criticality might be a vital property of healthy and functioning brain networks (Massobrio et al., 2015).

However, little is known about the functional significance and differences between criticality dynamics in different frequency bands. It has been shown that alpha (10 Hz) and beta (20 Hz) spontaneous oscillations are scale-free, with persistent power-law scaling ranging from 5 to 300 seconds. Moreover, it has been shown that the power-law scaling is significantly different for these oscillations, suggesting potentially different underlying mechanisms (K. Linkenkaer-Hansen et al., 2001). It has also been shown that midfrontal theta, known to be involved in action monitoring, is also scale-free (Cohen, 2016). Scale-free brain dynamics are found to be attenuated in a task compared to rest (He et al., 2010; Klaus Linkenkaer-Hansen et al., 2004), as well as strengthened (Borges et al., 2018; Ciuciu et al., 2008), suggesting that scaling analysis can reveal different aspects of task involvement. It has been shown that the scale-free amplitude modulation of gamma oscillations monotonically increases with accelerated speech rate, and gamma scale-free dynamics are therefore hypothesized to reflect cognitive load (Borges et al., 2018). Here we aim to investigate the impact of novelty on the scale-free amplitude modulation of narrow sub-bands of theta, beta and gamma neuronal oscillations in the hippocampal-cortical novelty detection circuit in mice.

Novelty and Exploration in Mice

Research on novelty dynamics in mice has indicated that hippocampal beta2 (23-30 Hz) power increases during the first couple of minutes of spatial and object novelty exposure (Berke et al.,

2008; França et al., 2014). Moreover, it has been demonstrated that hippocampal beta2 etrained cells rapidly gain spatial specificity during the first minutes of novelty exposure (Berke et al., 2008). Recently submitted work investigating hippocampal-cortical dynamics involved in the novelty detection circuit in mice has reported high coherence among the cortical regions (prefrontal and parietal cortices) and the hippocampus in beta2 frequency band during novelty. Notably, the coherence between the cortical regions is reported to be reduced after novelty exposure (França et al., n.d.).

The Current Study

The goal of this study is to examine the long range temporal correlations in free-moving mice during the exploration of novel and familiar objects. For this, local field potentials (LFP) were continuously recorded from the hippocampal-cortical circuit during task and rest, and in order to investigate the scaling properties of frequency-specific amplitude time series, Demeaned Fluctuation Analysis was applied (DMA). To our knowledge, this is the first project to examine long range temporal correlations in the mouse brain during novelty and familiarity. DMA is the most commonly used method to quantify scale-free behaviour in physiological data (Hardstone et al., 2012). With this method the so-called scaling exponent (α) is obtained, which is a measure of self-similarity for power law distributions, capturing the relationship of the data between different scales and is often interpreted as memory of the system. We verified that mice explore novel objects longer than familiar ones. We also found evidence for above-noise scale exponents in multiple frequency bands during rest and task, spanning between 0.6 and 1. Finally, we applied mixed-effects linear modeling to examine the contribution of the hippocampal-cortical circuit and behavioural outcome on the scaling exponents, and found evidence that regions and behavioural outcomes contribute differently to the scaling exponents in theta (4-7 Hz), beta2 (24-29 Hz) and gamma (96-102 Hz).

Methods

Data Acquisition and Animals

For this project 6 mice of two transgenic lines with a C57BL/6J background were used. The SST-Cre mouse line expressed Cre-recombinase in somatostatin-positive interneurons (4 mice in total), while PV-Cre mice expressed Cre in parvalbumin-positive interneurons (2 mice in total).

Local field potential (LFP) recordings with 32 channels were obtained from the prefrontal cortex (16 channels), parietal cortex (8 channels) and the hippocampus (8 channels, targeted at CA1) in 6 freely moving mice undergoing a one-trial object recognition task. The sampling rate of the

LFP recordings is 1000 Hz. Detailed information about the electrode hardware can be found in Franca et al (n.d.).

Experimental Procedure: One-Trial Object Recognition Task

The experiment was conducted by dr. Arthur Franca and his students from previous years.

The experiment consists of two main sessions - training and test. During each exploration stage, two objects were placed in a rectangular open field. Each session, training and test, consists of 3 stages: pre-exploration (home cage) followed by object exploration, and post exploration (home cage). The two object exploration stages of each session are termed “object training” and “object test” respectively. During object training, the two objects explored were identical, while during the object test, one of the previously explored objects was replaced by a novel one. The objects were placed in the same location of the field for each session. The setup of the experiment is illustrated in Figure 1, provided by dr. Arthur Franca.

The duration of the recordings from the pre- and post-exploration stages is 5 minutes, while the duration of each object exploration stage is 10 minutes. Both sessions of the experiment were

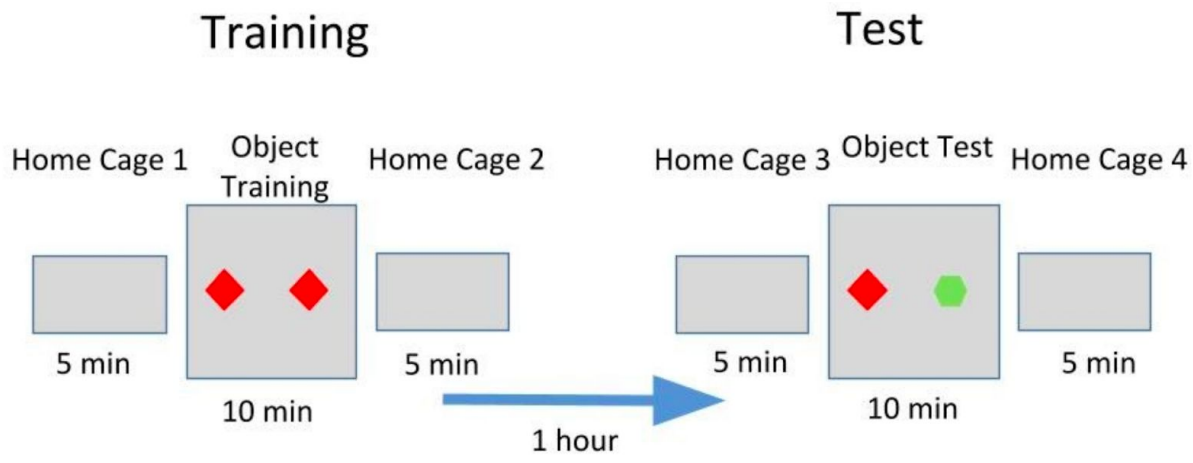

Figure 1: *Experimental Setup. Different color and shape signify difference in the objects shapes used in this experiment.*

recorded within the same day with a one hour time window between them. Each LFP data set is supported by a video recording of the same duration to monitor behaviour, sampled at 30 Hz.

Data Preprocessing

The LFP recordings were visually inspected for artifacts with the EEGLAB toolbox (Delorme & Makeig, 2004) in Matlab (R2019b). In this study, high amplitude sharp spikes were considered as artifacts and removed. For each data set, Independent Component Analysis (ICA) was performed using the routine runica from EEGLAB with the jader algorithm (Cardoso & Souloumiac, 1993). The ICA components identified to contain mainly artifacts were subtracted from each data set (the effect of the subtraction was first visually inspected). Channels were removed from a recording only if the component subtraction procedure did not completely remove all signal artifacts as defined above. Generally, this is the case when an electrode has detached from its original position.

Before proceeding to further steps in the analysis pipeline, region-wise normalization was performed by subtracting the mean of each region from the corresponding channels.

Frequency Decomposition

Narrow-band frequency decomposition was achieved by using Complex Morlet Wavelets. For each frequency, a Gaussian in the frequency domain (Morlet Wavelets in the time domain are Gaussians in the frequency domain) centered around the desired frequency was multiplied with the Fourier Transform of the data, and the Inverse Fourier Transform of the result was taken, which results in narrow band filtered signal. The time-frequency specificity of the wavelet is determined by the full-width at half-maximum (FWHM), a measure quantifying the width of the Gaussian at half amplitude in the frequency domain (Cohen, 2019). The FWHM parameter affects the frequency/time specificity ratio of the filtered signal.

For this work, frequencies between 2 Hz and 150 Hz were considered using linearly spaced FWHM between 2 Hz and 15 Hz. In the time domain these values translate to integration between 454ms and 60ms for the lowest and highest frequencies respectively.

Demeaned Fluctuation Analysis

Demeaned Fluctuation Analysis was first developed by Peng and colleagues (1994), and is implemented in this work as follows:

1. The signal profile was computed based on the demeaned cumulative sum of the amplitude envelope corresponding to each frequency. Figure 2A shows the amplitude envelope at 10 Hz from a single channel.
2. Twenty logarithmically spaced time scales were defined on the range between 1s and 30s.

3. Then, for each time scale:
    3.1. The signal profile was reconstructed via convolution with the corresponding time scale. The effect of the convolution is essentially smoothening the signal. The larger the time scale is, the more smoothened the reconstruction becomes relative to the signal profile obtained in step 1.
    3.2. Residuals were calculated by taking the difference between the signal profile and the corresponding reconstruction defined in step 3.1
    3.3. The scale fluctuation was obtained by rearranging the residuals times series into N adjacent non-overlapping windows, calculating the root square of each window and averaging across windows. The window size here corresponds to the length of the time scale used.
4. Steps 3.1 to 3.3 were repeated for each of the 20 time scales.
5. The fluctuations obtained for each scale were plotted on a log-log scale, and a line was fitted by means of linear regression.
6. The scaling exponent (α) is the slope of the fitted line. Figure 2B shows the resulting fluctuations against the scale sizes plotted on a log-log scale. The results shown in Figure 2B correspond to the amplitude envelope at 10 Hz illustrated on Figure 2A. The slope of the linearly fitted line corresponds to the resulting scaling exponent (0.69).

There is little consensus in the literature on the choice of scales duration and on the amount of scales to be considered. However, it is recommended that the shortest scale covers at least 4 data points, and the duration of the largest scale considered is no more than 10% of the total signal duration (Hardstone et al., 2012). As mentioned in the Experimental Procedure section, the duration of each object exploration stage is twice the length of the recordings obtained from the home cages. To be able to consistently compare the results from different experimental stages, we chose the longest scale to be 10% of the total duration of a home cage recording. To avoid temporal correlations induced by the narrow-band filtering, the shortest scale used in this study is chosen to be greater than the FWHM in the time domain of the wavelet used for extracting the lowest frequency (454 ms).

The scaling exponent α is also referred to as "self-similarity parameter" (Lux & Marchesi, 1999), which quantifies long-range temporal correlations across the signal. It can take values between 0 and 2, with the following interpretation:

- $\alpha \approx 1$ indicates the system is behaving at a critical point
- $\alpha > 1$ indicates the system is at a supercritical state. More specifically, $\alpha = 1.5$ is associated with Brownian Noise.
- $\alpha < 0.5$ indicates negative autocorrelation
- $\alpha > 0.5$ indicates positive autocorrelation with 1/f power spectrum
- $\alpha \sim 0.5$ indicates white noise - a random process with no memory,

In human neuroimaging data, signals resulting from power-law behaviour often result in scaling exponents (as assessed by Demeaned or Detrended Fluctuation Analysis) between 0.5 and 1 (Ghosh et al., 2018). Reports of scaling exponents from resting state M/EEG can be found, among others, in Linkenkaer-Hansen and colleagues (2001).

A)

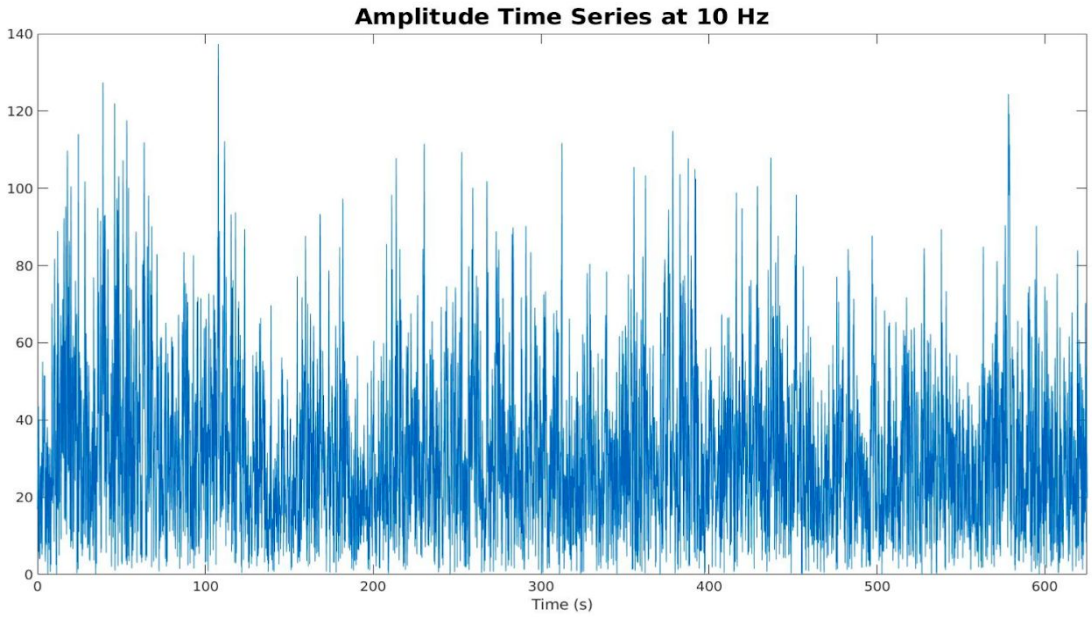

B)

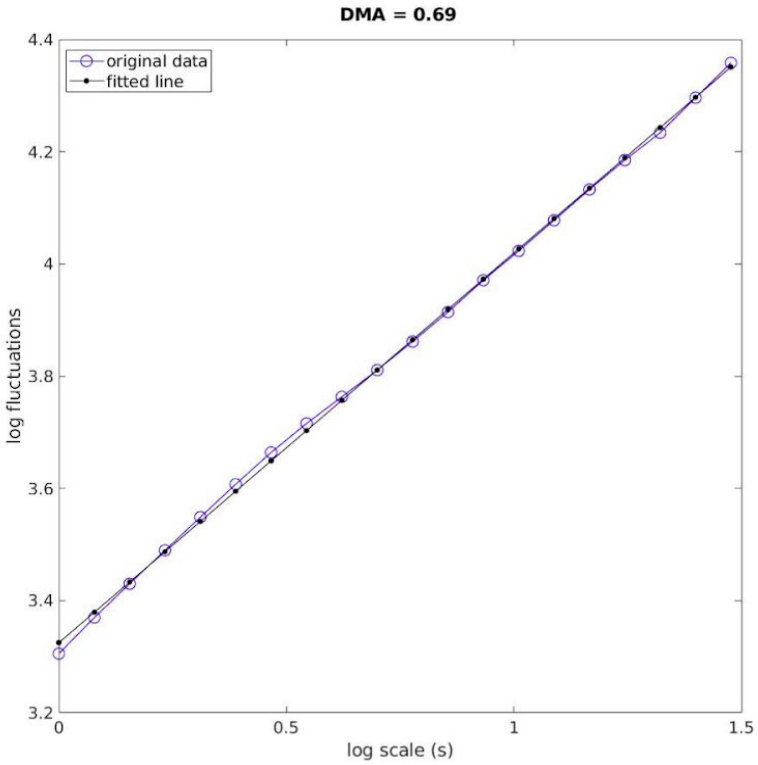

Figure 2: *A - Amplitude time series at 10 Hz from one animal (single channel); B - resulting fluctuation plotted against the scale sizes on a log-log scale. The slope of the linearly fitted line corresponds to the resulting scaling exponent (0.69).*

Influence of Filter Parameters on DMA Estimates

As mentioned in the previous section, the scaling exponent (α) for white noise is expected to be 0.5. However, it is known that filters (such as wavelets used for frequency extraction) can introduce autocorrelation, especially for low frequencies. Autocorrelation is a correlation function between the signal itself and its delayed copy. Procedures, such as frequency extraction via wavelet convolution inflate the autocorrelation for law frequencies because the wavelet is then very narrow in the frequency domain, and thus, signal leakage can occur in the time domain. To inspect the effects of the filter on the scaling exponent, DMA was applied for frequencies between 2 Hz and 150 Hz extracted from white noise with duration of 300s. This procedure was repeated for 500 times. The exponents associated with each frequency were then averaged. The results are summarized in Figure 3 and indicate that the frequency extraction procedure inflates the scaling exponents. This effect is most prominent for frequencies below 100 Hz. To account for this effect and to preserve the interpretation of the scaling exponents, we quantify the inflation introduced through the frequency extraction procedure as the difference between the noise simulation results and 0.5. Thus, the area under the curve in Figure 3 was subtracted from the DMA results.

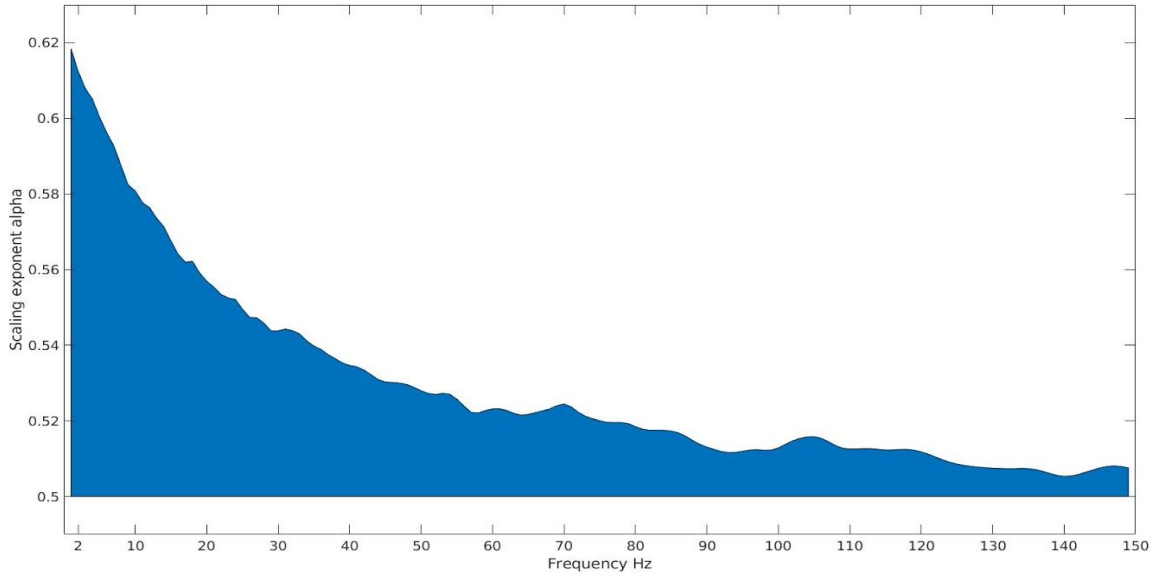

Figure 3*: Effect of frequency extraction on the scaling exponents.*

Linking Criticality to Behaviour

Sliding-Window Demeaned Fluctuation Analysis

The procedure for the sliding-window DMA is similar to the one described above. The main difference is that now, instead of a single scaling exponent, a time course of scaling exponents with the length of the original time series is obtained. This is achieved by sliding the time scales across the entire signal while computing the fluctuations of the DMA. The discrete time step of the sliding procedure is 2 data points. The range of scales used for this analysis is the same, namely logarithmically spaced scales of duration between 1s and 30s. For this analysis 15 scales were used per computation instead of 20.

The analysis was performed on selected channels within a region, and for the following frequency bands: Theta (4-7 Hz), Beta (24-29 HZ), and Gamma (96-102 Hz). To explore whether the hippocampus might be operating in distinct spatial networks, and that the operations of these networks could be reflected in the scaling exponents, the hippocampus was represented by two distinct sets of hippocampal channels. Channels used to represent each region are the following:

- Prefrontal cortex (PFC) - channels 9, 10, 11
- Parietal cortex (PAR) - channels 21, 22, 23, 24
- Hippocampus (HIP) - channels 27, 28, 29 and channels 30, 31, 32

The channels chosen to represent each region, as well as the width of each frequency sub-bands, are solely chosen based on the results obtained from the static DMA procedure, averaged across animals (Figure 6A, Results section).

Pose Estimation: DeepLabCut

To link the scaling exponents time courses to distinct behavioral outcomes, first, pose estimation is performed with DeepLabCut[1] (DLC, (Mathis et al., 2018)). DLC is a software package for markerless pose estimation based on deep neural networks. This software allows to track the location of predefined body parts of the animal from frame to frame. This analysis is performed only on the object exploration stages of the experiment, because the objective is to link scaling exponent with specific behavioural outcomes, such as object exploration vs free movement in the arena.

For each stage, training and test, 200 frames were labeled for the models' training. The body parts used for pose estimation are the following: left ear, right ear, nose and the beginning of the

[1] http://www.mousemotorlab.org/deeplabcut

tail. The corners of each object were also labeled and used in further analysis to determine whether the mouse was exploring an object or not. Figure 4 illustrates the points taken for animal tracking and defining the object boundaries with DLC. Two models (one per object exploration stage) were trained on the ResNet-101 network (convolutional neural network with 101 layers) with 200 000 iterations. The number of iterations during training is based on the observation that the network's performance does not improve above this threshold. Since the true performance rate of the DLC model is hard to estimate precisely due to the low resolution of the videos and lack of true labels, the model's performance was visually inspected by plotting the inferred coordinates on top of the original videos. It was observed that the model sometimes swaps the left and right ear coordinates of the mouse. To overcome this issue, the median of the mouse body parts was taken as a single estimate of the animal's position.

The threshold used for object exploration in this study was whether the animal is in the polygon derived from the object corners, that is, whether the upper body of the mouse is within the boundaries of the object. The derived behavioural categories are the following:

- Exploration - the animal is within the boundaries of any of the two object during object training
- Novelty - the animal is within the boundaries of a novel object during object test
- Familiarity - the animal is within the boundaries of a familiar object during object test

Finally, the behavioural categorizations were synchronized with the scaling exponents time courses based on the interpl1 function from Matlab. To avoid artifacts characteristic for vectors obtained through a sliding-window procedure, the last 1500 data points from each behavioral vector were disregarded, and the beginning of the computation was set to the first video frame free from the researcher.

For each animal, for each object exploration session, the scaling exponents at time t corresponding to a behavioural category were summed and averaged.

The video recording from one animal during object test was corrupted, and therefore the data from this experimental stage coming from this animal was excluded from further analysis.

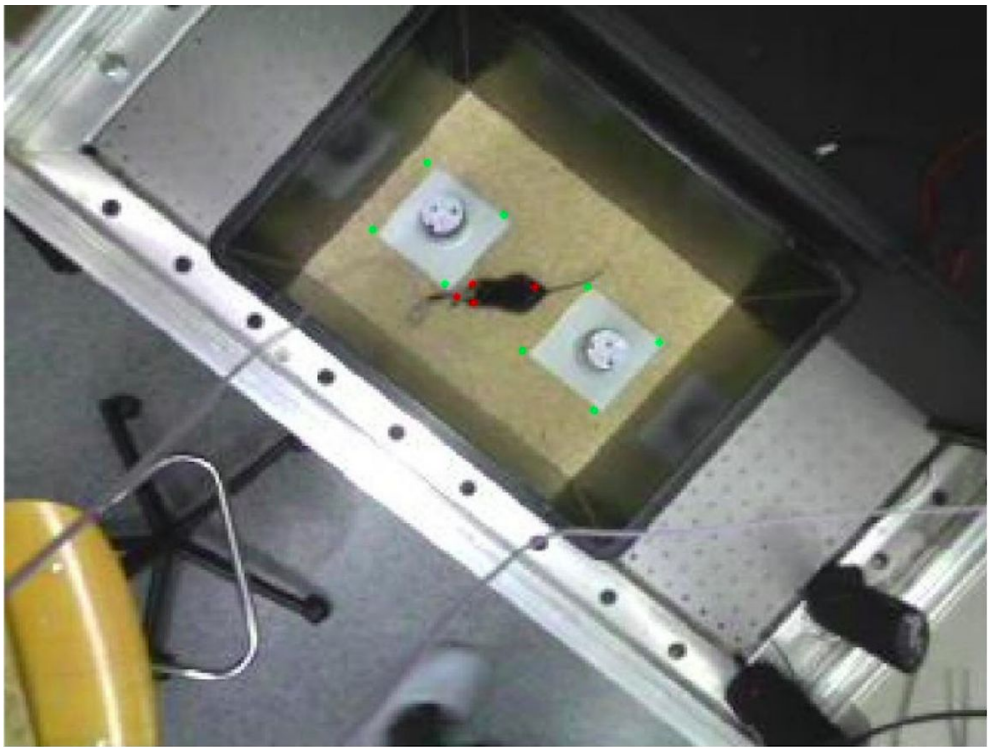

***Figure 4**: Coordinates used for animal tracking and behavioural analysis*

Mixed-Effects Linear Modeling

To examine the effect of the hippocampal-cortical circuit and the behavioural outcomes on the scaling exponents, linear-mixed effects models were independently constructed for each frequency band. To compare the scaling exponent dynamics between object exploration and rest, the average values within each frequency band and region from the home cage recordings were also included in the model.

The general linear mixed-effects models were fit to averaged within region estimates of the scaling exponents per frequency band with behavioural category and regions as independent variables and random intercepts and/or slopes per animal as the mixed effect component. To facilitate log-likelihood ratio tests, the models were fitted using the maximum likelihood method. The modeling was based on reference encoding for each predictor, setting the coefficients of the first level (in alphabetical order) of each predictor to zero. The reference for regions is thus the hippocampus, and for behavioural categories - exploration. Thus, the meaning of the intercepts is the average predicted scaling exponent for exploration in the hippocampus.

Model selection was based on the outcome of simulated likelihood ratio tests with 1000 simulations per test, as well as visual examination for violation of model assumptions (e.g., homoscedasticity, normality of residuals). The models chosen for each frequency band were the following:

- Theta: alpha~category + regions + category:regions + (1|animalID)
- Beta: alpha~category + regions + (1|animalID)
- Gamma: alpha ~ category + regions + (-1 + regions|animalID)

Here alpha is the obtained scaling exponent, and the terms in brackets is the random effects component. For theta and beta the random effects component is an individual intercept per animal, and in gamma it is individual regional dynamics per animal without separate individual intercepts.

Results

Behavioural Trends During Object Exploration

The animals spend roughly only 15% of their time actively exploring an object, while during the rest of the session the animals are engaged with non-exploratory activity. During object training, the animals explore the objects between 8% and 21% percent of the total duration of the session. During object test, the animals tend to spend, on average, around twice longer exploring a novel object compared to the familiar one. This is in line with previous reports on exploratory behaviour in rodents (Dere et al., 2007). Animals explore the novel object between 4% and 13% of the total duration of the session, while the familiar object is explored between 3% to 5% of the session's duration. The difference between animals on the time spent exploring objects cannot be attributed to genetic differences. However, one mouse explored the objects during training much less than its peers. This animal explored the objects for only 8% of its time, while its peers explored the objects for 10% to 21% of their time. Another animal spent in total 7% of its time on object exploration during the test session (3% on the familiar object, and 4% on the novel one), while the rest spent at least 11% of their time exploring objects. Figure 5 illustrates the average time spent on object exploration for each object exploration stage.

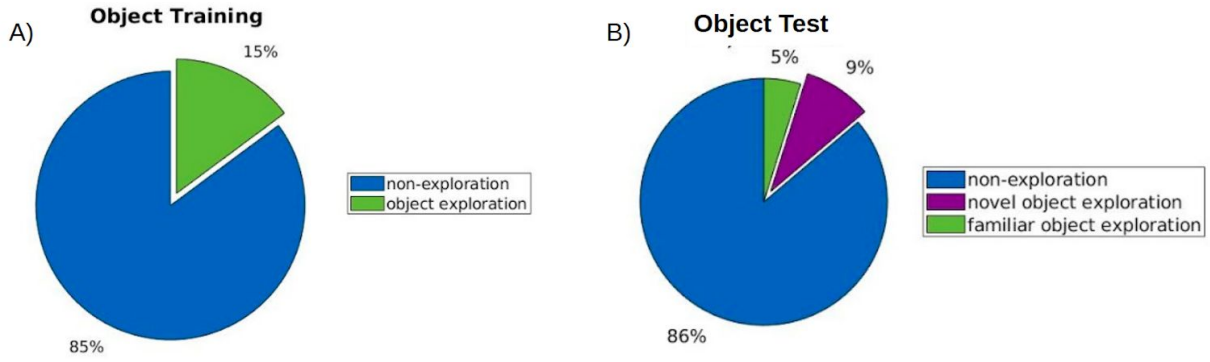

Figure 5: *Average behaviour during object exploration stages of the experiment. Panel A illustrates the behavioural trends for object training, Panel B shows the behavioural trends for object test.*

Above-Noise Scaling Exponents in the Mouse Brain

Figure 6A shows the scaling exponents per session averaged across all animals. The red dashed lines indicate regional boundaries. From left to right, the regions are prefrontal cortex (PFC), parietal cortex (PAR), and the hippocampus (HIP). Figure 6B shows a schematic representation of the electrode layout.

The most striking bursts of scaling exponents were observed in the parietal cortex for the gamma frequency band (~96-102 Hz) during object training and test experimental stages. The values of the scaling exponents for gamma during object training for this region vary, on average, between 0.59 and 0.86, and for object test - between 0.7 and 0.93. These gamma bursts in scaling exponents were most prominent during object exploration stages, however remained consistent during the rest of the experimental stages Figure 5A.

Smaller in magnitude, but yet relatively high bursts of scaling exponents were also observed in theta (~4-7 Hz) and beta (~24-29 Hz) in the parietal cortex during the two object exploration stages. The scaling exponents for theta and beta for this region vary, on average, between ~0.5 and ~0.6, with slightly higher values of scaling exponents during object test compared to object training. The bursts in scaling exponents in theta and beta were most prominent during object exploration stages, and, on average, were attenuated during the staying in home cages.

Bursts of higher scaling exponents were also found in the hippocampus during object exploration stages in theta and beta. The scaling exponents were slightly higher for object training in beta

compared to object test (ranges: [0.58 0.65] vs. [0.55 0.62]). This effect was observed to be the opposite for theta (object training: [0.53 0.58]; object test: [0.56 0.61]).

Interestingly, electrode 10, positioned in the prefrontal cortex (cingulate), displayed similar dynamics to the parietal cortex in terms of scaling exponents results.

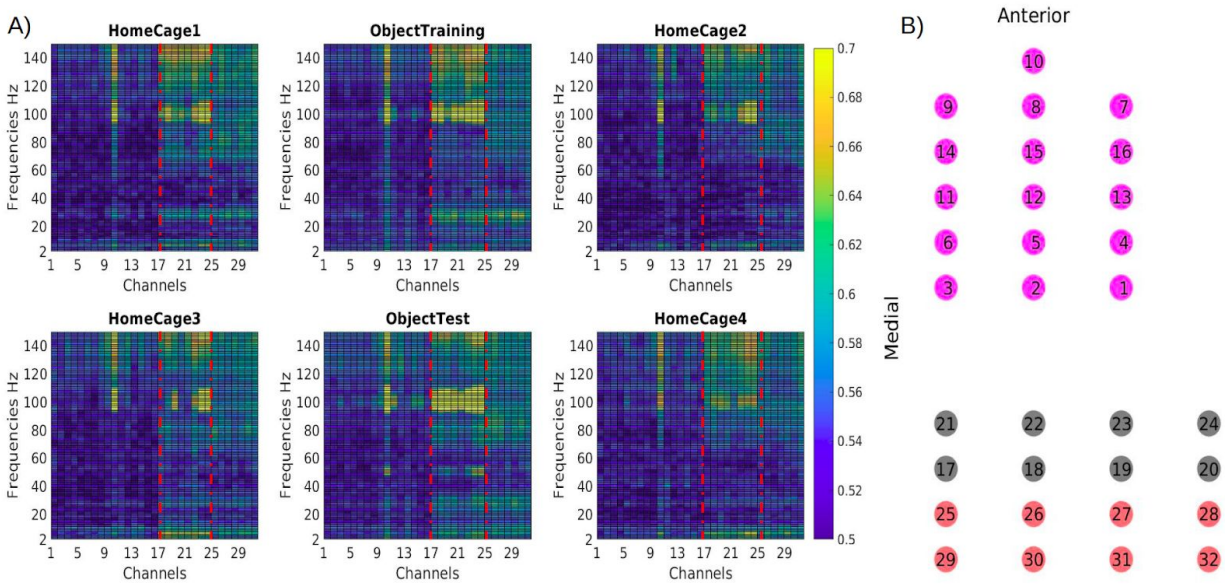

Figure 6: *Panel A - average (across animals) scaling exponents per experimental stage. The red dashed lines indicate regional boundaries. From left to right the regions are: prefrontal cortex (PFC), parietal cortex (PAR), and the hippocampus (HIP). Panel B shows a schematic representation of the electrode layout. The colour signify different region: magenta-PFC, gray - PAR, red - HIP*

Influence of Hippocampal Channels on the Scaling Exponents in Theta

The most prominent effect for the choice of hippocampal channels on the linear mixed effects model's (LMEs) inference can be observed in theta frequency band (4-7 Hz). Table 1 contains a summary of the most prominent differences in coefficient estimates between the two models. The coefficients are rounded up to four decimals. From here on, the model including hippocampal channels 27-29 will be referred to as model 1, and the model including hippocampal channels 30-32 as model 2.

One of the most striking differences between the two models lies in the effect of novelty on the prediction of the scaling exponents. In model 1, novelty raises the scaling exponents by 0.0541

compared to exploration, while in model 2 the scaling exponents for novelty are 0.0021 lower compared to exploration, and this effect is not significant. Moreover, the interaction between novelty and the parietal cortex brings a twofold increase in the scaling exponents in model 2 compared to model 1. A similar effect can be observed in the interaction between familiarity and the parietal cortex.

Another notable difference between the two theta models lies in familiarity. Even though the effect of familiarity is not significant compared to exploration in either of the models, in model 1 familiarity on average increases the scaling exponents, while in model 2, familiarity decreases them. Moreover, the scaling exponents in the prefrontal cortex are on average 0.0568 higher than in the hippocampus for model 1, while in model 2 the increase in scaling exponents due to prefrontal dynamics is not significant.

In both models, the increase in scaling exponents associated with the parietal cortex alone is not significant compared to the hippocampus. However, the contribution of the parietal cortex to the scaling exponents is higher for model 1 compared to model 2. Both models indicate no significant difference between the contribution of each of the cortical regions to the scaling exponents (p-value model 1: 0.4744; p-value model 2: 0.4498).

In both models the interaction between regions and behavioural categories is a significant term (p-value model 1: 0.0076204; p-value model 2: 2.3109e-05). Consistent between both models is the finding that the interaction between some home cage recordings and the prefrontal cortex significantly influence the prediction of scaling exponents by decreasing them by ~0.07 compared to the intercept (Table 2). Together, these results suggest that, from the view of criticality, there might be distinct hippocampal networks operating in the theta frequency band involved in the discrimination between novelty and familiarity. Moreover, scaling exponents in theta might also reflect a rather general mechanism involved in the coordination of information from multiple regions.

Theta Model 1 (HIP channels 27-29)				Theta Model 2 (HIP channels 30-32)			
Name	***Estimate***	***SE***	***pValue***	***Name***	***Estimate***	***SE***	***pValue***
(Intercept)	0.5809	0.0179	<0.01	(Intercept)	0.6031	0.0165	<0.01
category_familiar	0.0242	0.0245	>0.1	category_familiar	-0.0077	0.0232	>0.1
category_novel	0.0541	0.0245	<0.05	category_novel	-0.0022	0.0232	>0.1
category_home4	0.0215	0.0233	>0.1	category_home4	-0.0017	0.0221	>0.1
regions_PAR	0.0402	0.0233	<0.1	regions_PAR	0.0179	0.0221	>0.1
regions_PFC	0.0569	0.0233	<0.05	regions_PFC	0.0346	0.0221	>0.1
category_familiar: regions_PAR	0.0588	0.0346	<0.1	category_familiar: regions_PAR	0.0925	0.0327	<0.01
category_novel: regions_PAR	0.0402	0.0346	>0.1	category_novel: regions_PAR	0.0983	0.0327	<0.01
category_home4: regions_PAR	-0.0189	0.033	>0.1	category_home4: regions_PAR	0.0044	0.0312	>0.1
category_novel: regions_PFC	0.0049	0.0346	>0.1	category_novel: regions_PFC	0.0631	0.0327	<0.1
category_home1: regions_PFC	-0.0664	0.033	<0.05	category_home1: regions_PFC	-0.0578	0.0312	<0.1
category_home2: regions_PFC	-0.0571	0.033	<0.1	category_home2: regions_PFC	-0.0454	0.0312	>0.1
category_home3: regions_PFC	-0.0868	0.033	<0.01	category_home3: regions_PFC	-0.0756	0.0312	<0.05
category_home4: regions_PFC	-0.0954	0.033	<0.01	category_home4: regions_PFC	-0.0722	0.0312	<0.05

Table 1: *Summary of the coefficients for the theta models depending on hippocampal channels. In this table, coefficients are included either on the base of significance, or on the base of change in the estimate sign.*

Frequency Specific Differences in Contributions to the Scaling Exponents

Unlike in theta, in beta and gamma the choice of hippocampal channels did not have a significant effect on the models' inference. Table 2 provides a summary of both beta and gamma models fixed effects coefficients for hippocampal channels 27-29.

In both beta and gamma, the average scaling exponents for novelty are roughly ~0.0021 lower compared to exploration. However, this effect is significant in beta, while it is not in gamma. It is also interesting to note that only in theta with hippocampal channels 27-29 on average novelty increases the scaling exponents (relative to exploration), while in the rest of the models novelty attenuates them.

The effect of familiarity compared to exploration is significant only in beta frequency band, while it is not neither in gamma, nor in theta, regardless of the hippocampal channels. On average, compared to exploration, familiarity attenuates the scaling exponents by ~0.06 in beta, and by ~0.02 in gamma. There is no significant difference between the contribution of novelty and familiarity to the scaling exponents for any of the explored models (theta model 1 p-value: 0.2424, theta model 2 p-value: 0.8197, beta p-value: 0.7764, gamma p-value: 0.3537).

Compared to exploration, the scaling exponents from all home cage recordings are on average ~0.1 lower in beta frequency band (Table 2), and this effect is significant for all home cages. Similar effect, but to a lesser magnitude, is observed in gamma (Table 2), where the scaling exponents from home cages are on average ~0.05 lower compared to exploration. However, in gamma this effect is not significant for all home cage stages. Interestingly, in the gamma model with hippocampal channels 30-32, the attenuation in scaling exponents from home cages following object exploration is greater (roughly ~0.06), than for home cages preceding object exploration (roughly ~0.03). However, similar to the results in gamma with hippocampal channels 27-29, this effect is not significant for all home cage stages. In theta, the contribution of a home cage recording to the scaling exponents (relative to exploration) is not significant, regardless of the hippocampal channels. Together, these findings contradict previous results suggesting that scaling exponents decrease during task (He, 2011), but are in line with (Ciuciu et al., 2008). Our results suggest that scaling exponents in beta could reflect involvement in novelty detection.

Regions wise, the cortical regions are significantly different from each other in beta (p-value: 5.4868e-05) and gamma (p-value: 0.0046), while they are not in theta (see previous section). The scaling exponents for the parietal cortex in gamma are on average 0.07 higher compared to the hippocampus, and this contribution is significant only in this frequency band (Table 2), and

strongest in magnitude compared to beta and theta. In theta, the contribution of the parietal cortex is not significant, regardless of the hippocampal channels, however, the elevation of scaling exponents due to the parietal cortex is twofold stronger in magnitude in model 1 (Table 1). These results suggest that the scaling exponents in gamma (96-102 Hz) are primarily driven by the parietal cortex.

Interestingly, the contribution of the prefrontal cortex to the scaling exponents is significant in theta (hippocampal channels 27-29, Table 1) and beta (Table 2), but with an opposite effect. In theta, the prefrontal cortex increases the scaling exponents, while in beta this region attenuates them.

Beta model (HIP channels 27-29)				**Gamma model (HIP channels 27-29)**			
Name	***Estimate***	***SE***	***pValue***	***Name***	***Estimate***	***SE***	***pValue***
(Intercept)	0.6784	0.0137	<0.01	(Intercept)	0.6325	0.0178	<0.01
category_familiar	-0.0616	0.0117	<0.01	category_familiar	-0.0255	0.0233	>0.1
category_novel	-0.0582	0.0117	<0.01	category_novel	-0.003	0.0233	>0.1
category_home1	-0.0938	0.0111	<0.01	category_home1	-0.047	0.0221	<0.05
category_home2	-0.1325	0.0111	<0.01	category_home2	-0.0797	0.0221	<0.01
category_home3	-0.1106	0.0111	<0.01	category_home3	-0.0544	0.0221	<0.05
category_home4	-0.1237	0.0111	<0.01	category_home4	-0.0695	0.0221	<0.01
regions_PAR	0.0014	0.0075	>0.1	regions_PAR	0.0702	0.0252	<0.01
regions_PFC	-0.0298	0.0075	<0.01	regions_PFC	0.0218	0.0194	>0.1

Table 2: *Comparison of coefficients for beta and gamma models with hippocampal channels 27-29*

Individual Variability in Scaling Exponents

Figure 7A shows individual conditional expectation (ICE) plots for the random effects of the models for each frequency band. The results shown in this figure are from the models including hippocampal channels 27-29. The plots contain 21 lines (behavioural categories x regions), and show how each observation affects the prediction of the scaling exponent in each frequency band. The thick red lines illustrate the average effect an animal has on the prediction of the scaling exponents. The analysis of the random effects does not indicate any costincy between the frequency bands. In theta, the analysis indicates that the intercept for animal #346110 is significantly different from from the rest (p-value: 0.009); in beta - animal #339295 (p-value:

4.7898e-05); in gamma - cortical responses from animal #346111 are significantly different from the hippocampus (p-values: 0.0019). These results are preserved in the models including hippocampal channels 30-32.

Figure 7B shows the original data from each frequency band (with hippocampal channels 27-29) grouped by behavioural outcome, and color coded by regions. A striking observation is that the scaling exponents in gamma from the hippocampus are within a tight range (~0.5-0.65), while the scaling exponents from the cortical regions are more sparsely distributed. This is especially prominent for a few scaling exponents from the parietal cortex with values above 0.75. These scattered parietal scaling exponents come from 3 animals (#279419, #339295, #346111), and cannot be attributed to genetic differences. Interestingly, the characteristic bursts of scaling exponents in gamma (~96-102 Hz) in the parietal cortex, as evident from the averaged scaling exponents across animals in Figure 6A, are individually present only in these 3 animals. These bursts are most prevalent during the object exploration stages of the experiment, but also during Home Cage 1 and Home Cage 3 (these home cage recordings precede an object exploration stage). Only 1 animal out of these 3 (#346111) exhibits high gamma scaling exponents in this gamma sub-band in all experimental stages, and has the highest maximal scaling exponents compared to the other two animals. Notably, this is the same animal that was recognized by LMEs to have significantly different cortical influences on the prediction of the scaling exponents. The scaling exponents for this narrow gamma sub-band (96-102 Hz) across the entire parietal cortex in the three animals can reach values of ~1.05. This observation explains why the gamma scaling exponent bursts are so prominent in the averaged scaling exponent maps (Figure 6A) despite not being present in all animals.

Additionally, one more animal (#339296) displays high scaling exponents in a lower gamma sub-band (centered at ~80 Hz), also in the parietal cortex. For this animal, the scaling exponents vary between 0.5 and 0.7 across the entire cortical region. Moreover, all animals to a certain extent display high scaling exponents in broadband gamma (>100 Hz), which are not necessarily restricted to the parietal cortex. However, there does not seem to be any particular pattern in scaling exponents across animals. Whether the scaling exponents from different gamma sub-bands are functionally meaningful awaits future investigation. The individual patterns of scaling exponents per experimental stage can be found in the Appendix, Figure A1.

All animals show above noise-level scaling exponents in the beta range (~24-29 Hz) in the parietal cortex and the hippocampus, predominantly during the first home cage recording and during the object exploration stages (Figure A1 A-D). These experimental stages are most intense in contextual, spatial and/or object novelty. The scaling exponents for the animals vary between ~0.6 and ~0.7 across all parietal channels, and can reach ~0.8 across the hippocampus. This observation gives further support for the interpretation of beta scaling exponents as possibly reflecting the processing of novelty and/or exploratory behaviour. Moreover, the scaling

exponents for the somatostatin-positive animals are on average higher compared to the parvalbumin-positive ones, however, the LMEs did not indicate consistent significance based on genetic background.

Above noise-level scaling exponents are also present in the theta frequency range (~4-7 Hz) across all channels and all experimental stages in five out of six animals (in the remaining animal, above average scaling exponents are also present, but not in all channels/experimenta; stages). The scaling exponents for theta vary between 0.6 and ~0.86. The scaling exponents in this frequency range do not seem to majorly vary between regions. The maximum values of theta scaling exponents are evenly distributed across regions and experimental stages. These results point out that there is no clear regional specificity of theta scaling exponents when regions as a whole are taken into account. This is also partially supported by the results of the LME including hippocampal channels 30-32. In this model, neither of the cortical regions was estimated to have significantly different contributions in the scaling exponents compared to the hippocampus (Table 2).

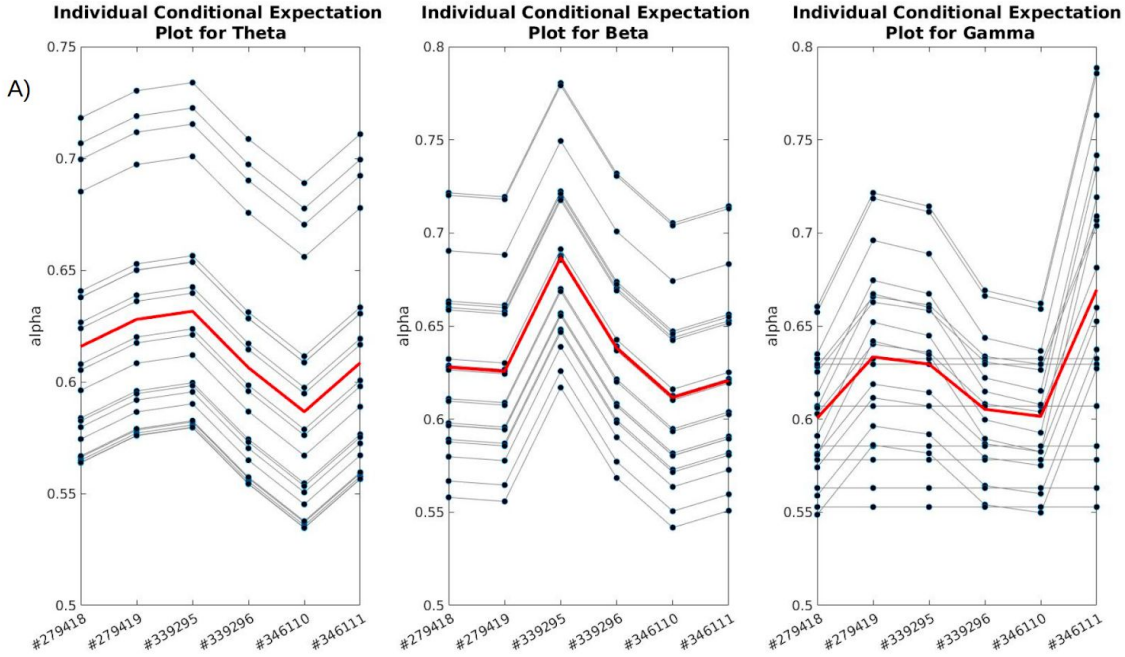

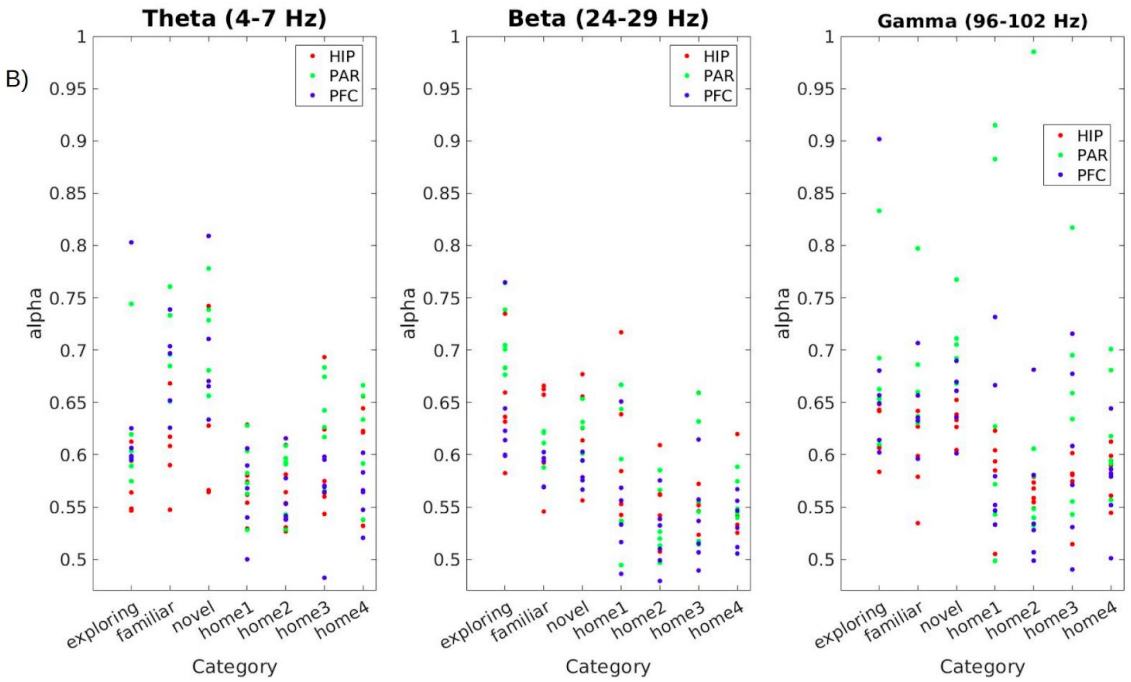

Figure 7: *Panel A* ***-*** *Individual Condition Expectation Plots showing responses from individual animals for each frequency band. The thick red line shows the average effect an animal has on the prediction of the scaling exponents; Panel B - distribution of scaling exponents grouped by behavioural category and region across animals for each frequency band. The results in both sub-figures are from the datasets including hippocampal channels 27-29.*

Discussion

In this study we found support for the presence of long range temporal correlation in the mouse brain during object recognition spanning from 1s to 30s in multiple frequency bands. To our knowledge, this is the first piece of research investigating the scaling dynamics of continuous oscillatory activity during object recognition in rodents.

Our results indicate that the scaling exponents associated with exploration in the hippocampus are the highest in beta frequency band (23-29 Hz). Moreover, the greatest attenuation of scaling exponents in magnitude for rest compared to task was observed in beta. Together with previous research linking the role of beta entrained place cells on rapidly obtained spatial specificity (Berke et al., 2008), and increased beta power during exposure to novelty (Berke et al., 2008; França et al., 2014), our results suggest that the scaling exponents in beta could be reflecting cognitive processes involved in novelty detection. Alternatively, beta scaling exponents might also be linked to anxiety. While there is no comprehensive research on this topic, especially

investigating the effect of anxiety on the long range temporal correlations of oscillatory activity, some (unpublished) research has shown increased beta power and altered theta/beta synchrony associated with anxiety (Cruces-Solis et al., n.d.). There is also an alternative theory suggesting that functional neuronal networks operate at a "reverbating regime", which enables networks to tune to task demands. According to this theory, only networks which need to integrate information over multiple time scales will be operating at a critical regime (Wilting et al., 2018). If this is the case, then the hypothesis that the scaling exponents in beta reflect novelty detection and exploratory behaviour seems to be more plausible than the anxiety hypothesis. Moreover, if the beta scaling exponents would be reflecting anxiety levels, it is reasonable to hypothesize that throughout the experiment the anxiety levels would drop, which would in turn be reflected in the scaling dynamics (e.g., decrease in scaling exponents during object test session). Another piece of research supporting our interpretation of the functional significance of criticality in beta comes from scale-free analysis of inter-spike intervals of interneurons in the mouse hippocampus (CA1 region) during slow wave sleep and free exploration. The authors report an increase of ~0.1 in scaling exponents during exploration compared to slow-wave sleep, however, the observed changes in scaling properties were not formally tested for significance (Guo et al., 2007). Whether our results of increased scaling exponents in beta truly reflect involvement in novelty detection or alternatively, increased levels of anxiety, awaits future investigation.

Our work also provides evidence that different hippocampal sides could be contributing differently to the scaling properties of theta (4-7 Hz) frequency band associated with novelty. To our knowledge, this is the first piece of evidence to demonstrate that hippocampal subregions can potentially contribute differently to the long-range temporal correlations of continuous oscillatory activity. However, these results need to be validated through better channel selection in the analysis pipeline. In the current work, channels representing a region were solely selected based on the averaged scaling exponent maps, and anatomical proximity was not taken into account. This poses constraints on the validity and the interpretation of these results, however, our research already gives novel evidence for potentially different scaling regimes in theta across the CA1 region of the hippocampus. Regardless of the choice of hippocampal channels, our results indicate that only in theta frequency band the interaction between regions and behavioral outcomes significantly influences the scaling dynamics. Consistent across both models is the finding that the interactions of two out of four home cage recordings with the prefrontal cortex significantly decrease the scaling exponents by ~0.07. In humans, theta oscillations have been implicated to play a crucial role in working memory (Stam, 2000) and are hypothesized to integrate information in inter-regional networks involved in mnemonic tasks (Kirk & Mackay, 2003). Moreover, midfrontal theta, implicated in action monitoring in humans, has been shown to be scale free (Cohen, 2016). It has also been shown that long-range temporal correlations in patients with major depressive disorder (a symptom of which is memory impairment) in theta from multiple sources is nearly absent, while it is robust in healthy participants (Klaus Linkenkaer-Hansen et al., 2005). In rodents (rats) it has been previously shown that the neuronal

firing of the prefrontal cortex is phase-locked to hippocampal (CA1) theta rhythm (Siapas et al., 2005), and that increased phase-locking of the prefrontal cortex to hippocampal theta is associated with increased working-memory loads and/or decision making (Jones & Wilson, 2005). Therefore we hypothesize that theta scaling properties might reflect a rather general mechanism involved in the coordination of information from multiple regions associated with memory in the object recognition task.

The greatest variability in scaling exponents was observed in the gamma frequency band. In the averaged across animals scaling exponent maps, prominent gamma (~96-102 Hz) scaling exponent bursts were observed during object exploration stages, spanning on average between 0.6 and 0.93. Interestingly, only three out of six animals contributed to these prominent scaling dynamics, and in these animals the scaling exponents were observed to reach values above 1. Additionally, one more animal showed similar scaling dynamics for a lower gamma sub-band (centered around ~80 Hz). These results cannot be attributed to genetic differences and suggest that possibly different underlying mechanisms are contributing to the scaling properties of gamma. Contrary to our expectations, these prominent bursts of scaling exponents were found in the parietal cortex. The parietal cortex in mice has been implicated to take part in various tasks, such as processing different modalities of sensory information (Mohan et al., 2018; Olcese et al., 2013), resolving conflicts of sensory information coming from different modalities (Song et al., 2017), and decision-making and navigation (Harvey et al., 2012; Krumin et al., 2018). Therefore the prominent bursts in scaling exponents found in the parietal cortex might reflect a multitude of mechanisms involved in the object recognition task. However why the results indicate prominent above-noise level scaling exponents in the narrow gamma sub-band (~96-102 Hz), and what is the possible interpretation for the generally high scaling exponents observed in broad gamma (>100 Hz) awaits future investigation.

Interestingly, channel 10 from the prefrontal cortex, positioned at the cingulate, displayed strikingly similar scaling dynamics to those observed in the parietal cortex. There is research indicating the presence of reciprocal connections between the parietal cortex and the anterior cingulate cortex in the mouse brain (Zingg et al., 2014). Moreover, the anterior cingulate cortex has been implicated to take part in the novelty detection circuit in mice (Weible et al., 2009). Therefore it is plausible to hypothesize that the similarity in scaling properties between these two regions reflect both connectivity and general involvement of these regions in the task. Whether this is the case awaits future investigation. Another plausible interpretation for the similarity of scaling dynamics between the cingulate and the parietal cortices is the possibility for short-circuit on the electrode level. Even though all data was carefully preprocessed for artifacts, it is still possible that short-circuits have significantly contributed to the remaining signal. Whether the similarity in scaling dynamics between the cingulate and the parietal cortices is due to short circuits or is alternatively due to strong connectivity between these regions and reflects a general network involved in the object recognition task awaits future investigation.

A limitation of the current work lies in the experimental design. In this work mice were not habituated to the open field before being exposed to novel objects. Therefore, our behavioural category "exploration" encodes not only object novelty, but also spatial novelty, and it is impossible to compare the scaling properties of neural oscillations associated with each of the two types of novelty. Another strong limitation of the current work is that the chosen modelling framework (LMEs) does not allow for the formal testing for significance between the intercepts of each model. Our results that the scaling exponents associated with exploration in the hippocampus are the highest in beta are not supported with a formal significance test. Comparison of the intercepts for significance is possible in linear regression models with the same slopes, and in a seemingly unrelated regression model, where the individual regressions are allowed to have different slopes. However, both of the above mentioned models do not allow for the explicit specification of the random effects, as it is done in this work. Moreover, the linear mixed effects models might not be the most optimal modelling paradigm to investigate the difference between the scaling dynamics associated with each behavioural outcome. This is reflected in the relatively low R-squared (a measure of the variance explained) for each model. The highest R-squared is ~0.7 for the beta models, in theta this measure is ~0.6 and in the gamma models - only ~0.4. The relatively low R-squared in gamma could partially be attributed to the wider range of scaling exponents observed within this frequency sub-band. This might suggest that there are different, conquering processes, independently contributing to the scaling exponents within gamma. However, whether this is the case awaits future investigation.

A future direction would be to explore the long-range temporal correlations of other low frequency bands, such as delta and alpha. Individual scaling exponent maps, as well as the averaged results across sessions give preliminary support for the presence of scale-free amplitude modulations in the lower end of the frequency spectrum. Moreover, Figure 2B gives preliminary support for the presence of long-range temporal correlations in alpha (10 Hz). The results demonstrated there (from a single channel in the parietal cortex, from one randomly selected animal during object test) are strikingly similar to the ones reported by Linkenkaer-Hansen and colleagues (2001; 2004). Moreover, a recently submitted work investigating cross-frequency coupling during spatial and object novelty in mice has provided evidence for transient delta-beta coupling during exposure to novelty. (França et al., n.d.). Therefore, it will be interesting to investigate whether the scaling properties of these frequencies are also similar during the object recognition task.

Acknowledgements

Throughout this project I have learned a lot not only about the theory of criticality in the brain, but I have also developed on a personal level. I have learned to be persistent in my work, no

matter whether I am personally encouraged by the results or not, and I have improved my critical thinking. I would like to thank my supervisor dr. Michael Cohen for his guidance throughout my research internship, encouragement, support and motivating me to continue. I would also like to thank dr. Arthur Franca for the help in interpretation of my results and suggestions, Ashutosh Mishra for helping me to get acquainted with DeepLabCut and dr. Bernhard Englitz for setting up access for me to more powerful machines, which greatly accelerated the behavioral categorization part of this work. Last but not least, I would like to thank all of my friends who were forced to listen in great detail about my work and didn't break their friendship with me after that.

References

Bak, P., Tang, C., & Wiesenfeld, K. (1987). Self-organized criticality: An explanation of the 1/fnoise. In *Physical Review Letters* (Vol. 59, Issue 4, pp. 381–384). https://doi.org/10.1103/physrevlett.59.381

Bak, P., Tang, C., & Wiesenfeld, K. (1988). Self-organized criticality. In *Physical Review A* (Vol. 38, Issue 1, pp. 364–374). https://doi.org/10.1103/physreva.38.364

Beggs, J. M., & Plenz, D. (2003). Neuronal avalanches in neocortical circuits. *The Journal of Neuroscience: The Official Journal of the Society for Neuroscience*, *23*(35), 11167–11177.

Berke, J. D., Hetrick, V., Breck, J., & Greene, R. W. (2008). Transient 23-30 Hz oscillations in mouse hippocampus during exploration of novel environments. *Hippocampus*, *18*(5), 519–529.

Borges, A. F. T., Giraud, A.-L., Mansvelder, H. D., & Linkenkaer-Hansen, K. (2018). Scale-Free Amplitude Modulation of Neuronal Oscillations Tracks Comprehension of Accelerated Speech. In *The Journal of Neuroscience* (Vol. 38, Issue 3, pp. 710–722). https://doi.org/10.1523/jneurosci.1515-17.2017

Cardoso, J. F., & Souloumiac, A. (1993). Blind beamforming for non-gaussian signals. In *IEE Proceedings F Radar and Signal Processing* (Vol. 140, Issue 6, p. 362). https://doi.org/10.1049/ip-f-2.1993.0054

Carlson, J. M., Chayes, J. T., Grannan, E. R., & Swindle, G. H. (1990). Self-organized criticality in sandpiles: Nature of the critical phenomenon. *Physical Review. A*, *42*(4), 2467–2470.

Christensen, K., Danon, L., Scanlon, T., & Bak, P. (2002). Unified scaling law for earthquakes. *Proceedings of the National Academy of Sciences of the United States of America*, *99 Suppl*

1, 2509–2513.

Ciuciu, P., Abry, P., Rabrait, C., & Wendt, H. (2008). Log Wavelet Leaders Cumulant Based Multifractal Analysis of EVI fMRI Time Series: Evidence of Scaling in Ongoing and Evoked Brain Activity. In *IEEE Journal of Selected Topics in Signal Processing* (Vol. 2, Issue 6, pp. 929–943). https://doi.org/10.1109/jstsp.2008.2006663

Cohen, M. X. (2016). Midfrontal theta tracks action monitoring over multiple interactive time scales. *NeuroImage*, *141*, 262–272.

Cohen, M. X. (2019). A better way to define and describe Morlet wavelets for time-frequency analysis. *NeuroImage*, *199*, 81–86.

Cruces-Solis, H., Babaev, O., Ali, H., Chatain, C. P., Mykytiuk, V., Balekoglu, N., Wenger, S., & Krueger-Burg, D. (n.d.). *Altered theta / beta frequency synchrony links abnormal anxiety-related behavior to synaptic inhibition in Neuroligin-2 knockout mice*. https://doi.org/10.1101/726190

Delorme, A., & Makeig, S. (2004). EEGLAB: an open source toolbox for analysis of single-trial EEG dynamics including independent component analysis. *Journal of Neuroscience Methods*, *134*(1), 9–21.

Dere, E., Huston, J. P., & De Souza Silva, M. A. (2007). The pharmacology, neuroanatomy and neurogenetics of one-trial object recognition in rodents. In *Neuroscience & Biobehavioral Reviews* (Vol. 31, Issue 5, pp. 673–704). https://doi.org/10.1016/j.neubiorev.2007.01.005

França, A. S. C., Borgegius, N., & Cohen, M. X. (n.d.). *Beta2 oscillations in the hippocampal-cortical novelty detection circuit*. https://doi.org/10.1101/2020.06.15.151969

França, A. S. C., do Nascimento, G. C., Lopes-dos-Santos, V., Muratori, L., Ribeiro, S., Lobão-Soares, B., & Tort, A. B. L. (2014). Beta2 oscillations (23-30 Hz) in the mouse

hippocampus during novel object recognition. In *European Journal of Neuroscience* (Vol. 40, Issue 11, pp. 3693–3703). https://doi.org/10.1111/ejn.12739

Franca, A. S. C., van Hulten, J. A., & Cohen, M. X. (n.d.). *Low-cost and versatile electrodes for extracellular chronic recordings in rodents*. https://doi.org/10.1101/2020.02.06.937201

Friedman, N., Ito, S., Brinkman, B. A. W., Shimono, M., DeVille, R. E. L., Dahmen, K. A., Beggs, J. M., & Butler, T. C. (2012). Universal critical dynamics in high resolution neuronal avalanche data. *Physical Review Letters*, *108*(20), 208102.

Ghosh, D., Sengupta, R., Sanyal, S., & Banerjee, A. (2018). Musicality of Human Brain through Fractal Analytics. In *Signals and Communication Technology*. https://doi.org/10.1007/978-981-10-6511-8

Guo, S.-B., Wang, Y., Yan, X., Lin, L., Tsien, J., & Huang, D.-S. (2007). Long-Range Temporal Correlations in the Spontaneous in vivo Activity of Interneuron in the Mouse Hippocampus. In *Advanced Intelligent Computing Theories and Applications. With Aspects of Artificial Intelligence* (pp. 1339–1344). https://doi.org/10.1007/978-3-540-74205-0_137

Hardstone, R., Poil, S.-S., Schiavone, G., Jansen, R., Nikulin, V. V., Mansvelder, H. D., & Linkenkaer-Hansen, K. (2012). Detrended fluctuation analysis: a scale-free view on neuronal oscillations. *Frontiers in Physiology*, *3*, 450.

Harvey, C. D., Coen, P., & Tank, D. W. (2012). Choice-specific sequences in parietal cortex during a virtual-navigation decision task. *Nature*, *484*(7392), 62–68.

He, B. J. (2011). Scale-free properties of the functional magnetic resonance imaging signal during rest and task. *The Journal of Neuroscience: The Official Journal of the Society for Neuroscience*, *31*(39), 13786–13795.

He, B. J., Zempel, J. M., Snyder, A. Z., & Raichle, M. E. (2010). The temporal structures and

functional significance of scale-free brain activity. *Neuron*, *66*(3), 353–369.

Jiang, L., Sui, D., Qiao, K., Dong, H.-M., Chen, L., & Han, Y. (2018). Impaired Functional Criticality of Human Brain during Alzheimer's Disease Progression. *Scientific Reports*, *8*(1), 1324.

Jones, M. W., & Wilson, M. A. (2005). Theta Rhythms Coordinate Hippocampal–Prefrontal Interactions in a Spatial Memory Task. In *PLoS Biology* (Vol. 3, Issue 12, p. e402). https://doi.org/10.1371/journal.pbio.0030402

Kirk, I., & Mackay, J. (2003). The Role of Theta-Range Oscillations in Synchronising and Integrating Activity in Distributed Mnemonic Networks. In *Cortex* (Vol. 39, Issues 4-5, pp. 993–1008). https://doi.org/10.1016/s0010-9452(08)70874-8

Krumin, M., Lee, J. J., Harris, K. D., & Carandini, M. (2018). Decision and navigation in mouse parietal cortex. *eLife*, *7*. https://doi.org/10.7554/eLife.42583

Lai, M.-C., Lombardo, M. V., Chakrabarti, B., Sadek, S. A., Pasco, G., Wheelwright, S. J., Bullmore, E. T., Baron-Cohen, S., MRC AIMS Consortium, & Suckling, J. (2010). A shift to randomness of brain oscillations in people with autism. *Biological Psychiatry*, *68*(12), 1092–1099.

Linkenkaer-Hansen, K., Monto, S., Rytsälä, H., Suominen, K., Isometsä, E., & Kähkönen, S. (2005). Breakdown of long-range temporal correlations in theta oscillations in patients with major depressive disorder. *The Journal of Neuroscience: The Official Journal of the Society for Neuroscience*, *25*(44), 10131–10137.

Linkenkaer-Hansen, K., Nikouline, V. V., Palva, J. M., & Ilmoniemi, R. J. (2001). Long-range temporal correlations and scaling behavior in human brain oscillations. *The Journal of Neuroscience: The Official Journal of the Society for Neuroscience*, *21*(4), 1370–1377.

Linkenkaer-Hansen, K., Nikulin, V. V., Palva, J. M., Kaila, K., & Ilmoniemi, R. J. (2004). Stimulus-induced change in long-range temporal correlations and scaling behaviour of sensorimotor oscillations. *The European Journal of Neuroscience*, *19*(1), 203–211.

Lux, T., & Marchesi, M. (1999). Scaling and criticality in a stochastic multi-agent model of a financial market. In *Nature* (Vol. 397, Issue 6719, pp. 498–500). https://doi.org/10.1038/17290

Malamud, B. D., Morein, G., & Turcotte, D. L. (1998). Forest fires: An example of self-organized critical behavior. *Science*, *281*(5384), 1840–1842.

Maslov, S., Paczuski, M., & Bak, P. (1994). Avalanches and 1/f noise in evolution and growth models. *Physical Review Letters*, *73*(16), 2162–2165.

Massobrio, P., de Arcangelis, L., Pasquale, V., Jensen, H. J., & Plenz, D. (2015). Criticality as a signature of healthy neural systems. *Frontiers in Systems Neuroscience*, *9*, 22.

Mathis, A., Mamidanna, P., Cury, K. M., Abe, T., Murthy, V. N., Mathis, M. W., & Bethge, M. (2018). DeepLabCut: markerless pose estimation of user-defined body parts with deep learning. In *Nature Neuroscience* (Vol. 21, Issue 9, pp. 1281–1289). https://doi.org/10.1038/s41593-018-0209-y

Maxim, V., Sendur, L., Fadili, J., Suckling, J., Gould, R., Howard, R., & Bullmore, E. (2005). Fractional Gaussian noise, functional MRI and Alzheimer's disease. *NeuroImage*, *25*(1), 141–158.

Mohan, H., de Haan, R., Mansvelder, H. D., & de Kock, C. P. J. (2018). The posterior parietal cortex as integrative hub for whisker sensorimotor information. *Neuroscience*, *368*, 240–245.

Moran, J. K., Michail, G., Heinz, A., Keil, J., & Senkowski, D. (2019). Long-Range Temporal

Correlations in Resting State Beta Oscillations are Reduced in Schizophrenia. *Frontiers in Psychiatry / Frontiers Research Foundation*, *10*, 517.

Olcese, U., Iurilli, G., & Medini, P. (2013). Cellular and synaptic architecture of multisensory integration in the mouse neocortex. *Neuron*, *79*(3), 579–593.

Pritchard, W. S. (1992). The brain in fractal time: 1/f-like power spectrum scaling of the human electroencephalogram. *The International Journal of Neuroscience*, *66*(1-2), 119–129.

Shew, W. L., Yang, H., Yu, S., Roy, R., & Plenz, D. (2011). Information capacity and transmission are maximized in balanced cortical networks with neuronal avalanches. *The Journal of Neuroscience: The Official Journal of the Society for Neuroscience*, *31*(1), 55–63.

Siapas, A. G., Lubenov, E. V., & Wilson, M. A. (2005). Prefrontal phase locking to hippocampal theta oscillations. *Neuron*, *46*(1), 141–151.

Song, Y.-H., Kim, J.-H., Jeong, H.-W., Choi, I., Jeong, D., Kim, K., & Lee, S.-H. (2017). A Neural Circuit for Auditory Dominance over Visual Perception. *Neuron*, *93*(5), 1236–1237.

Stam, C. J. (2000). Brain dynamics in theta and alpha frequency bands and working memory performance in humans. *Neuroscience Letters*, *286*(2), 115–118.

Usher, M., Stemmler, M., & Olami, Z. (1995). Dynamic pattern formation leads to 1/f noise in neural populations. *Physical Review Letters*, *74*(2), 326–329.

Ville, D. V. D., Van De Ville, D., Britz, J., & Michel, C. M. (2010). EEG microstate sequences in healthy humans at rest reveal scale-free dynamics. In *Proceedings of the National Academy of Sciences* (Vol. 107, Issue 42, pp. 18179–18184). https://doi.org/10.1073/pnas.1007841107

Watkins, N. W., Pruessner, G., Chapman, S. C., Crosby, N. B., & Jensen, H. J. (2016). 25 Years

of Self-organized Criticality: Concepts and Controversies. In *Space Science Reviews* (Vol. 198, Issues 1-4, pp. 3–44). https://doi.org/10.1007/s11214-015-0155-x

Weible, A. P., Rowland, D. C., Pang, R., & Kentros, C. (2009). Neural correlates of novel object and novel location recognition behavior in the mouse anterior cingulate cortex. *Journal of Neurophysiology*, *102*(4), 2055–2068.

Wilting, J., Dehning, J., Neto, J. P., Rudelt, L., Wibral, M., Zierenberg, J., & Priesemann, V. (2018). Operating in a Reverberating Regime Enables Rapid Tuning of Network States to Task Requirements. In *Frontiers in Systems Neuroscience* (Vol. 12). https://doi.org/10.3389/fnsys.2018.00055

Zingg, B., Hintiryan, H., Gou, L., Song, M. Y., Bay, M., Bienkowski, M. S., Foster, N. N., Yamashita, S., Bowman, I., Toga, A. W., & Dong, H.-W. (2014). Neural Networks of the Mouse Neocortex. In *Cell* (Vol. 156, Issue 5, pp. 1096–1111). https://doi.org/10.1016/j.cell.2014.02.023

Appendix

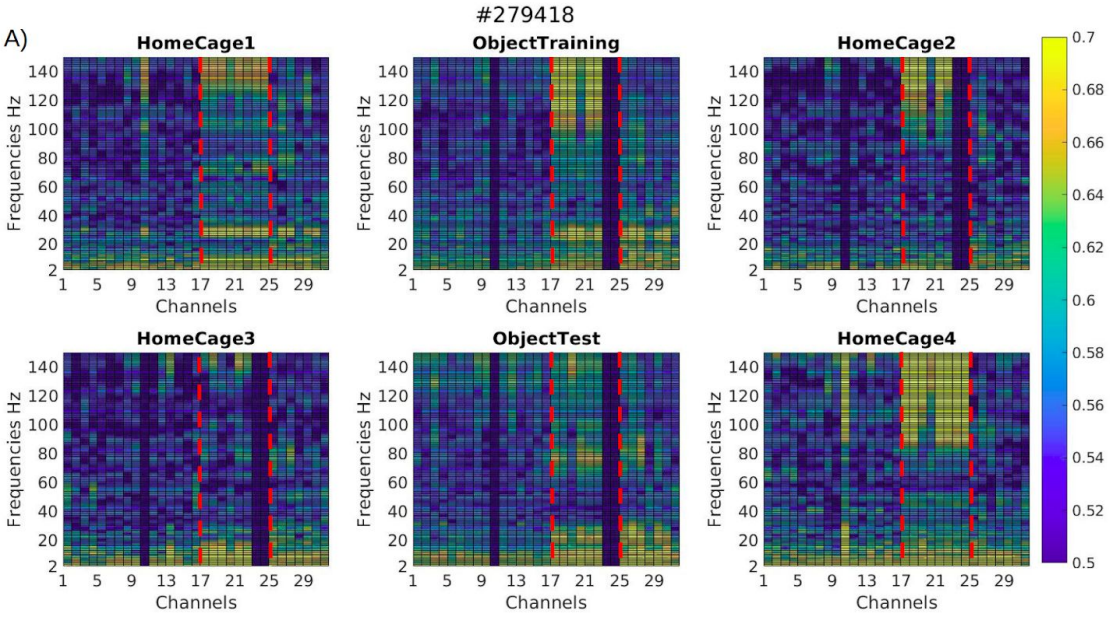
#279418
A)
HomeCage1
ObjectTraining
HomeCage2
HomeCage3
ObjectTest
HomeCage4
Frequencies Hz
Channels
0.7
0.68
0.66
0.64
0.62
0.6
0.58
0.56
0.54
0.52
0.5

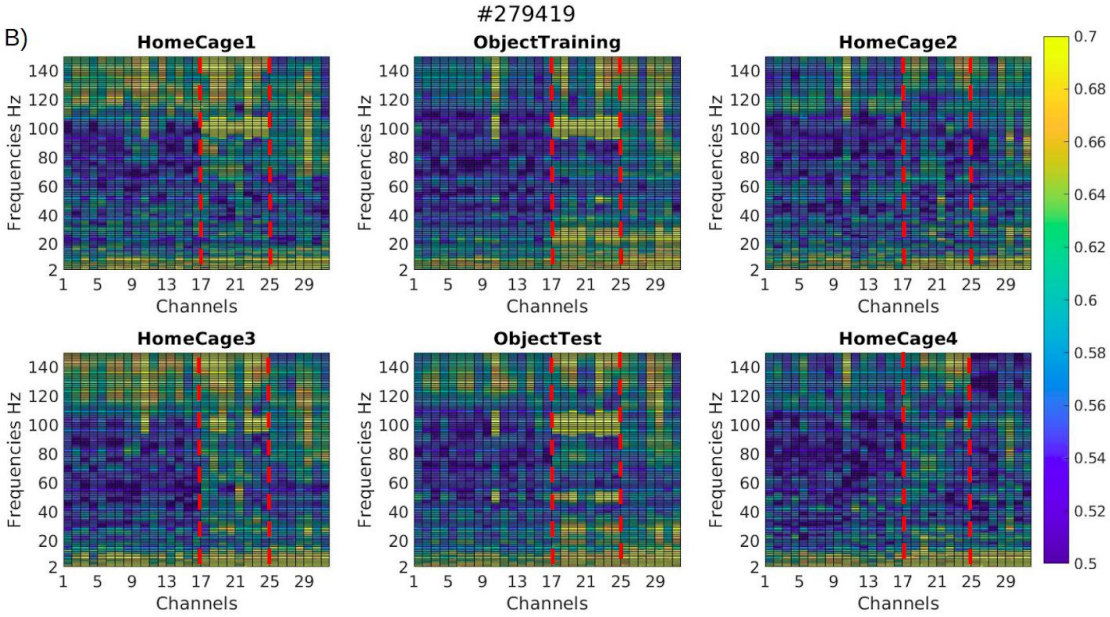
#279419
B)
HomeCage1
ObjectTraining
HomeCage2
HomeCage3
ObjectTest
HomeCage4
Frequencies Hz
Channels
0.7
0.68
0.66
0.64
0.62
0.6
0.58
0.56
0.54
0.52
0.5

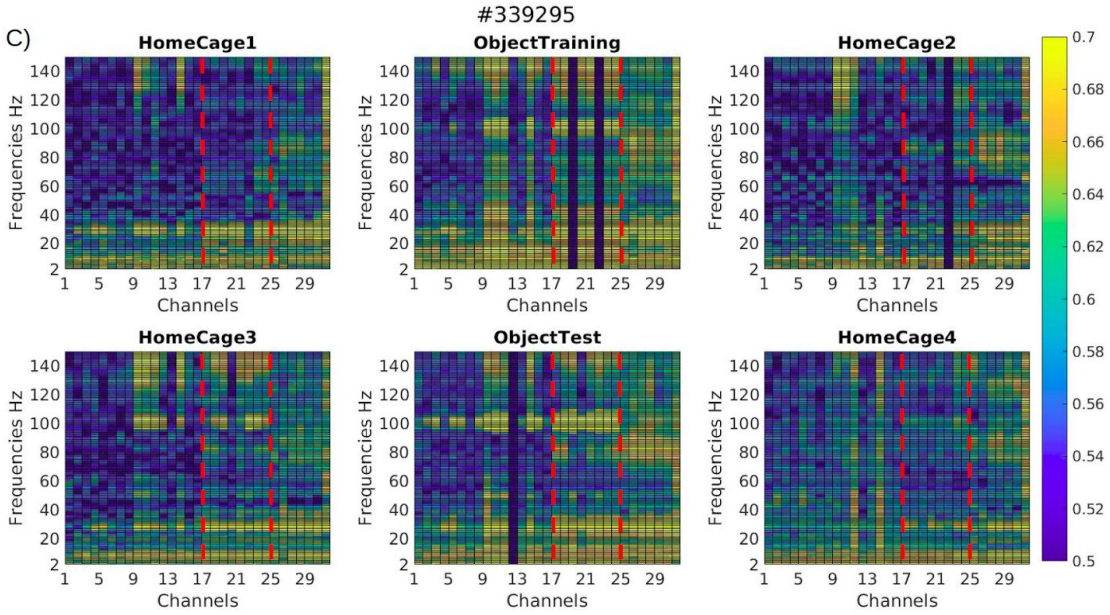
C)
#339295
HomeCage1
ObjectTraining
HomeCage2
HomeCage3
ObjectTest
HomeCage4
Frequencies Hz
Channels
0.7
0.68
0.66
0.64
0.62
0.6
0.58
0.56
0.54
0.52
0.5

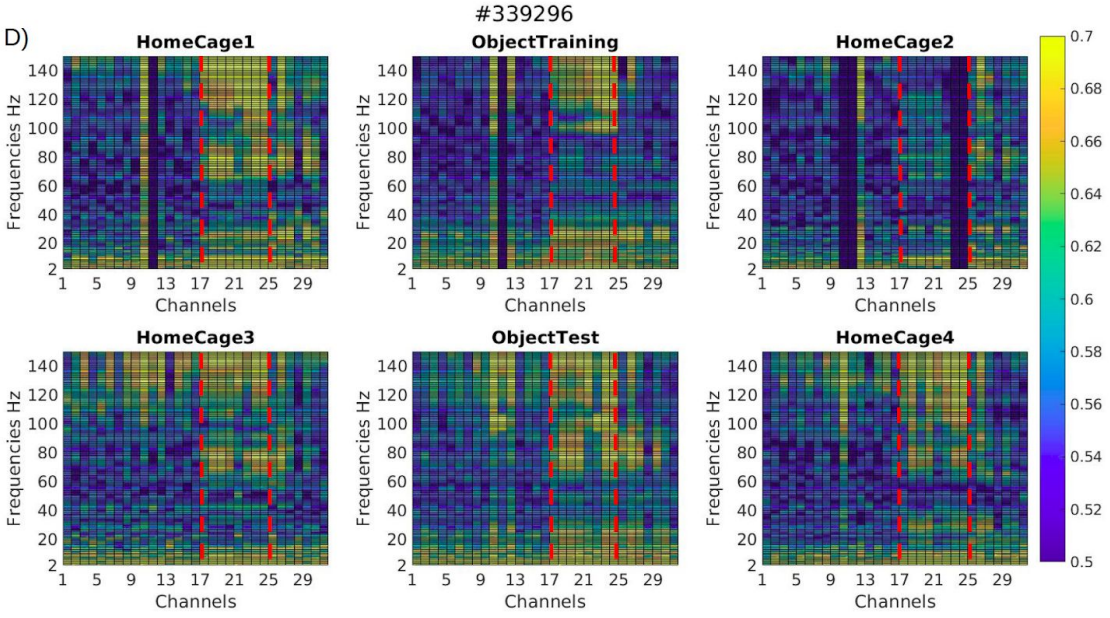
D)
#339296
HomeCage1
ObjectTraining
HomeCage2
HomeCage3
ObjectTest
HomeCage4
Frequencies Hz
Channels
0.7
0.68
0.66
0.64
0.62
0.6
0.58
0.56
0.54
0.52
0.5

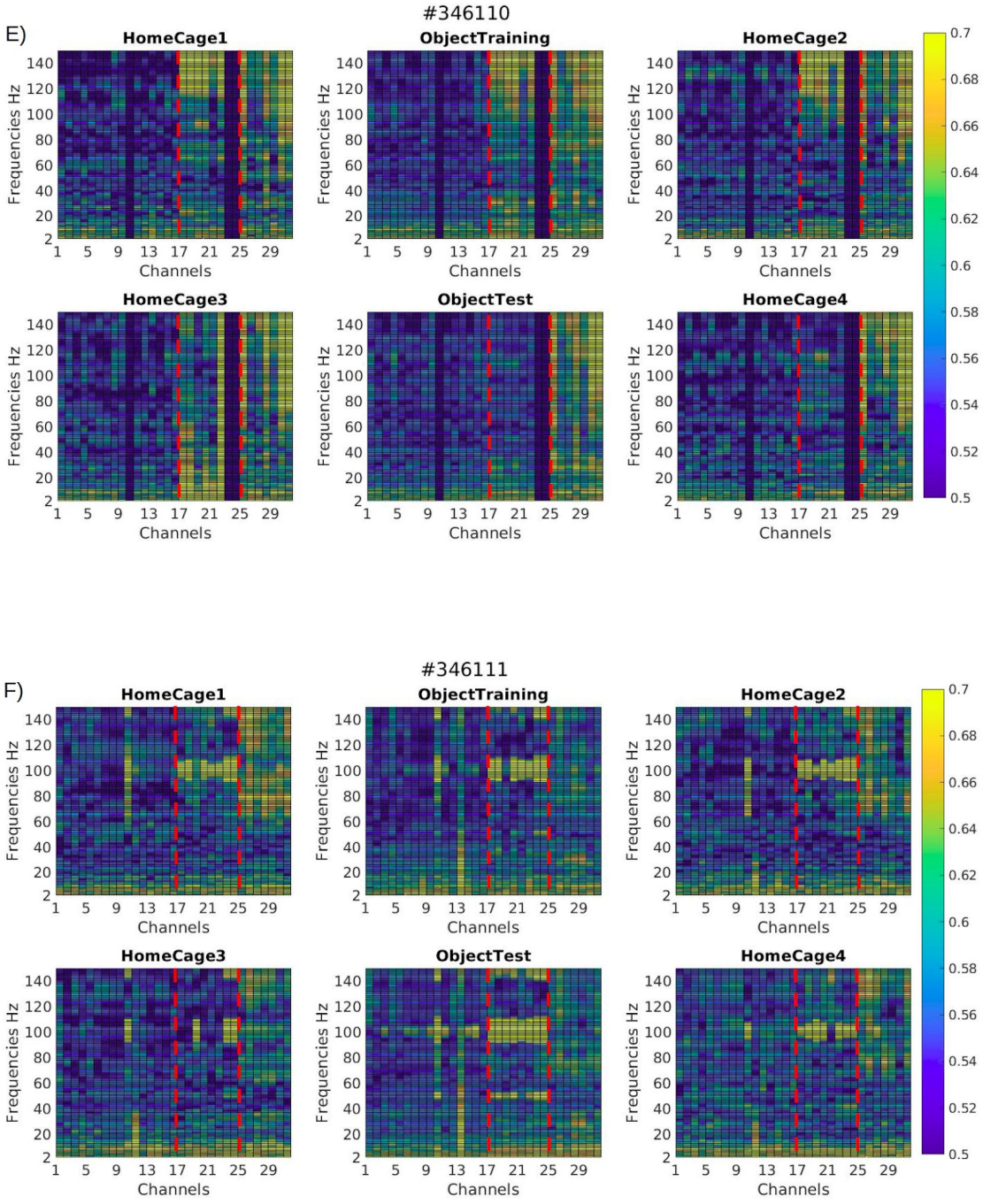

Figure A1*: Individual patterns of scaling exponents per experimental stage.*